

Developing Fragility Curves for Concrete Bridges Retrofitted with Steel Jacketing

Steel Jacket으로 보강된 콘크리트 교량에 대한 지진취약도 개발

김 상 훈
Kim, Sang Hoon

국문요약

본 연구의 궁극적인 목표는 콘크리트 교량의 교각을 Steel Jacket으로 보강한 효과를 정량적으로 산정함으로써, 지진 발생시 도로/교통 시스템의 역할을 평가할 수 있는 자료를 제공하는 데에 있다. Steel Jacket으로 보강 시, 교각의 연성능력이 어느 정도 증가되는지, 또 그로 인해 교량의 취약 상태가 어느 정도 개선되는지를 취약도 곡선을 통하여 나타내었다. 본 연구에서 해석적으로 구한 취약도 곡선이, 과거 지진 발생시 수집된 손상 자료를 이용하여 작성된 보강이 안 된 교량의 취약도 곡선을 보정하는데 사용하였다. 그 보정은 Steel Jacket 보강 전과 후의 취약도 곡선상의 중간 값들을 비교해 그 증가분 만큼을 반영하는 방식으로 수행되었다.

주요어 : 취약도곡선, Steel Jacket, 보강, 연성계수, 비선형동적해석

ABSTRACT

The ultimate goal of this research is to improve highway system performance in earthquakes by evaluating the effectiveness of retrofitting bridges with column jacketing. The objective of the study is to determine if steel jacketing increases the ductility capacity of bridge columns and hence improves the fragility characteristics of the bridge. Analytical fragility curves are used to adjust the empirical fragility curves obtained for the unretrofitted bridges using seismic damage data collected following past earthquakes. The adjustment was carried out by increasing the median values of the empirical curves through comparison with the median values of the corresponding fragility curves obtained analytically, both before and after being retrofit.

Key words : fragility curve, steel jacket, retrofit, ductility factor, nonlinear dynamic analysis

1 Introduction

Several recent destructive earthquakes, particularly the 1989 Loma Prieta and 1994 Northridge earthquakes in California, and the 1995 Kobe earthquake in Japan, have caused significant damage to highway structures. The investigation of this damage gave rise to a serious review of existing seismic design philosophies and led to extensive research activities on the retrofit of existing bridges as well as the development of seismic design methods for new bridges. This study presents an approach to the fragility assessment of bridges retrofitted by steel jacketing of columns with substandard seismic characteristics.

This study presents the results of an in-depth fragility analysis of typical bridges in California that have been strengthened using steel jacketing of bridge columns. A computer code was developed and used to calculate bilinear hysteretic parameters of the bridge columns before and after steel jacketing. Nonlinear dynamic time history analysis was used to evaluate the responses of the bridges before and after column retrofit under sixty ground acceleration

time histories developed for the Los Angeles area by the Federal Emergency Management Agency(FEMA) SAC(SEAOC ATC-CUREe) steel project(Somerville et al., 1997). Monte Carlo simulation was used to study fragility curves represented by lognormal distribution functions with two parameters (fragility parameters consisting of median and log-standard deviation) and developed as a function of peak ground acceleration(PGA). Fragility curves of the bridges before and after column retrofit were compared and the results show that steel jacketing improved the seismic performance of bridges.

2. Retrofit of the concrete columns

Concrete columns commonly lack flexural strength, flexural ductility and shear strength, especially in the bridges designed under older codes. The main causes of these structural inadequacies are lap splices in critical regions and/or premature termination of longitudinal reinforcement.

A number of column retrofit techniques, such as steel jacketing, wire pre-stressing and composite material jacketing have been developed and tested. Although advanced composite materials and other methods have been recently

학회원 · (주)대우건설 토목기술팀 차장(대표이사 : khs1210@chol.com)
본 논문에 대한 토의를 2003년 12월 31일까지 학회로 보내 주시면 그 결과를 게재하겠습니다.
(논문접수일 : 2003. 7. 5 / 심사종료일 : 2003. 8. 12)

studied, steel jacketing is the most common retrofit technique.

An experiment was performed by Chai et al.⁽¹⁾ to investigate the retrofit of circular columns with steel jacketing. In this experiment, for circular columns, two half shells of steel plate rolled to a radius slightly larger than the column are positioned over the area to be retrofitted and are site-welded up the vertical seams to provide a continuous tube with a small annular gap around the column. This gap is grouted with pure cement. Typically, the jacket is cut to provide a space of about 50mm(2 inches) between the jacket and any supporting member. This is to prevent the possibility of the jacket acting like a compressing reinforcement by bearing against the supporting member at large drift angles. The jacket is effective only in passive confinement and the level of confinement depends on the hoop strength and stiffness of the steel jacket.

3. Moment-curvature relationship

3.1 Confining effect of transverse reinforcement

Chai et al.⁽¹⁾ also observed that confinement of the concrete columns can be improved if transverse reinforcement layers are placed relatively close together along the longitudinal axis by restraining the lateral expansion of the concrete. This makes it possible for the compression zone to sustain higher compression stresses and much higher compression strains before failure occurs. Unfortunately, however, it can not be applied to existing bridges to enhance the performance of columns by adding transverse reinforcement layers.

3.2 Compression stress-strain relationship for confined concrete

Confinement increases the compression strength and

ultimate strain of concrete. Many different stress-strain relationships have been developed for confined concrete. Most of these are applicable under certain conditions. A recent model applicable to all cross-sectional shapes and all levels of confinement⁽²⁾ is used here for the analysis together with key equations from Priestley et al.⁽³⁾

4. Bridge Analysis

4.1 Description of bridges

Two example bridges used for the analysis are shown in Fig. 1 and 2. Bridge 1 has the overall length of 34m with three spans. The superstructure consists of a longitudinally reinforced concrete deck slab 10m wide and is supported by two pairs of columns (and by an abutment at each end). Each pair has three columns of circular cross section with 0.76m diameter. The overall length of Bridge 2 is 242m with five spans, with an expansion joint in the center span. This bridge is supported by four columns of equal height of 21m between the abutments at the ends. Each column has a circular cross section of 2.44m diameter. The deck has a three-cell concrete box type girder section 13m wide and 2m deep.

A column is modeled as an elastic zone with a pair of plastic zones at each end of the column. Each plastic zone is then modeled to consist of a nonlinear rotational spring and a rigid element depicted in Fig. 3. The plastic hinge formed in the bridge column is assumed to have bilinear hysteretic characteristics. For Bridge 2, the expansion joint is constrained in the relative vertical movement, while freely allowing horizontal opening movement and rotation. The closure at the joint, however, is restricted by a gap element when the relative motion of adjacent decks exhausts the initial gap width of 2.54cm.⁽⁴⁾ A hook element sustaining tension only is used for the bridge retrofitted by

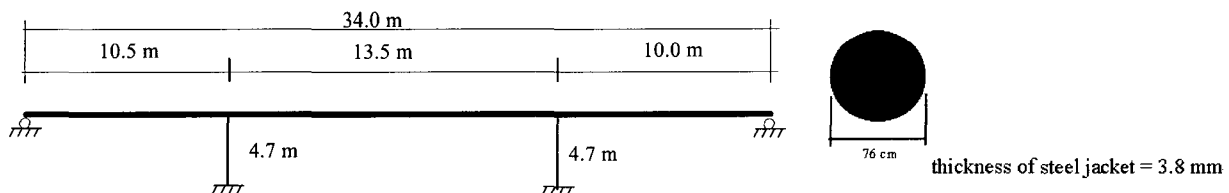


Fig. 1 Elevation and column section of Bridge 1

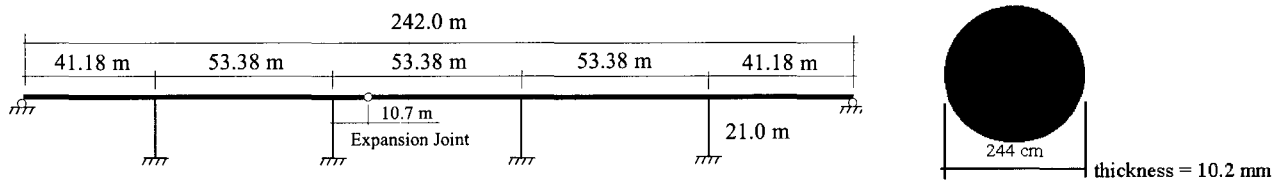


Fig. 2 Elevation and column section of Bridge 2

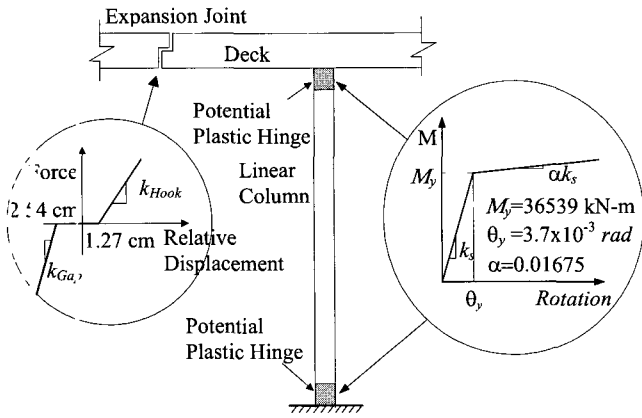


Fig. 3 Nonlinearities in bridge model

restainers at expansion joints and the opening is restricted by the element when the relative motion exhausts the initial slack of 1.27cm. Springs are also attached to the bases of the columns to account for soil effects, while two abutments are modeled as roller supports. To reflect the cracked state of a concrete bridge column for the seismic response analysis, an effective moment of inertia is employed, making the period of the bridge correspondingly longer.

4.2 Thickness of steel jacketing

The thickness of the steel jacket is calculated from the following equation.⁽³⁾

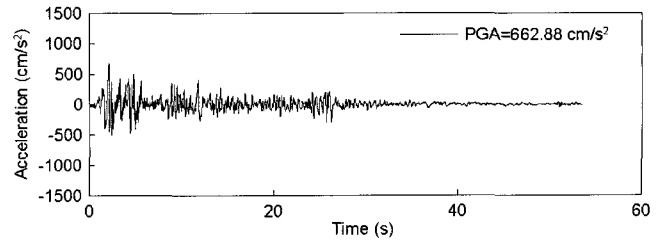
$$t_j = \frac{0.18(\epsilon_{cm} - 0.004)Df'_{cc}}{f_{yj} \epsilon_{sm}} \quad (1)$$

where ϵ_{cm} is the strain at maximum stress in concrete, ϵ_{sm} is the strain at maximum stress in steel jacket, D is the diameter of circular column, f'_{cc} is the compressive strength of confined concrete and f_{yj} is the yield stress of steel jacket.

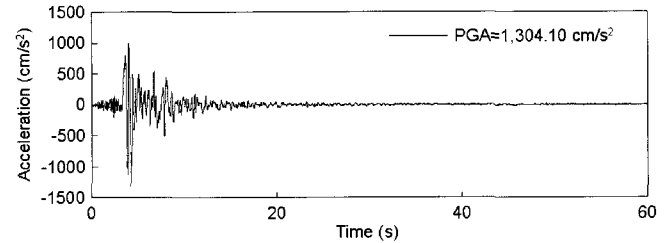
4.3 Nonlinear dynamic analysis

Nonlinear time history analysis has been performed using SAP2000 Nonlinear⁽⁵⁾ for the example bridges under sixty Los Angeles earthquake time histories(selected for FEMA SAC project) to develop fragility curves before and after column retrofitting the column with the steel jacket.

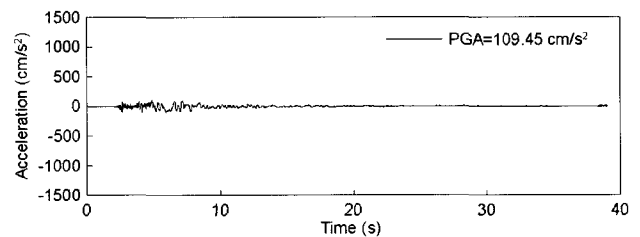
These acceleration time histories were derived from past records with some linear adjustments and consist of three groups(each with 20 time histories) with probabilities of exceedence of 10% in 50 years, 2% in 50 years and 50% in 50 years, respectively. A typical acceleration time history in each group is plotted in the same scale to compare the magnitude of the acceleration in Fig. 4.



(a) 10% Probability of Exceedence in 50 Years



(b) 2% Probability of Exceedence in 50 Years



(c) 50% Probability of Exceedence in 50 Years

Fig. 4 Acceleration Time Histories Generated for Los Angeles

4.4 Moment-curvature curves and damage states

Nonlinear response characteristics associated with the bridge are based on moment-curvature curve analysis taking axial loads as well as confinement effects into account. The moment-curvature relationship used in this study for the nonlinear spring is bilinear without any stiffness degradation. Its parameters are established using the computer code developed by Kushiyama^{(6),(7)} and by Caltrans(COLx).

These moment-curvature curves for a column of Bridge 1 are plotted together in Fig. 5. In the present study Kushiyama's curves are used for the dynamic analysis. The result shows that the curve after retrofit gives a much better performance than before retrofit by 2.6 times based on curvature at the ultimate compressive strain(or curvature).

The parameter used to describe the nonlinear structural response in this study is the ductility demand. The ductility demand is defined as θ/θ_y , where θ is the rotation of a bridge column in its plastic hinge under earthquake ground motion considered and θ_y is the corresponding rotation at the yield point.

A set of five different damage states is also introduced following the Dutta and Mander⁽⁸⁾ recommendations. These five damage states and the corresponding drift limits for a

typical column are given in Table 1. For each limit state, the drift limit can be transformed to peak ductility capacity of the columns for the purpose of this study. Table 2 lists the values for Bridges 1 and 2. The values for Bridge 1 are also shown in Fig. 5 for easy understanding.

Details for section of the column, stress-strain relationship, distribution of axial force, *P-M* interaction diagram, moment-curvature curve and moment-rotation curve for a column before and after retrofit are given in Shinozuka et al..⁽²⁾

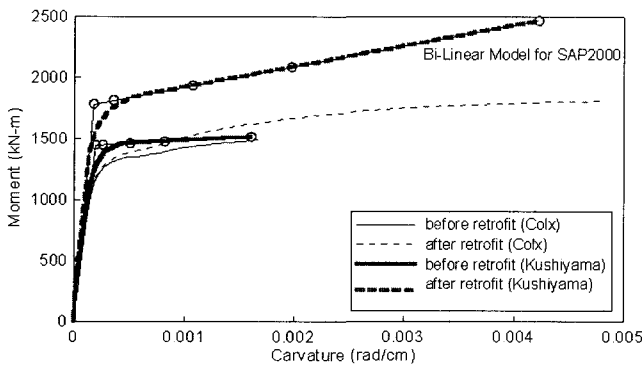


Fig. 5 Moment-curvature curves for column of Bridge 1

Table 1 Description of damage states

Damage state	Description	Drift limits
Almost no	First yield	0.005
Slight	Cracking, spalling	0.007
Moderate	Loss of anchorage	0.015
Extensive	Incipient column collapse	0.025
Complete	Column collapse	0.05

Table 2 Peak ductility demand of columns of example bridges

Damage State	Bridge 1		Bridge 2	
	before retrofit	after retrofit	before retrofit	after retrofit
Almost no	1.0	1.0	1.0	1.0
Slight	1.4	2.4	1.5	2.3
Moderate	3.1	7.9	3.5	7.5
Extensive	5.3	14.8	6.0	14.3
Complete	10.7	32.1	12.3	30.9

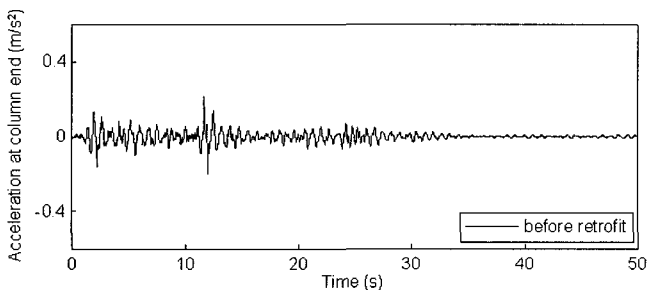
4.5 Bridge response

Typical responses at column bottom end of Bridge 1 are plotted in Fig. 6. As expected, the rotation after retrofit is generally smaller than before, while the accelerations do not necessarily behave similarly and are quite different each other. Some higher fluctuations in the acceleration response appear after retrofit because the column becomes stiffer than before. The same trend is observed for Bridge 2.

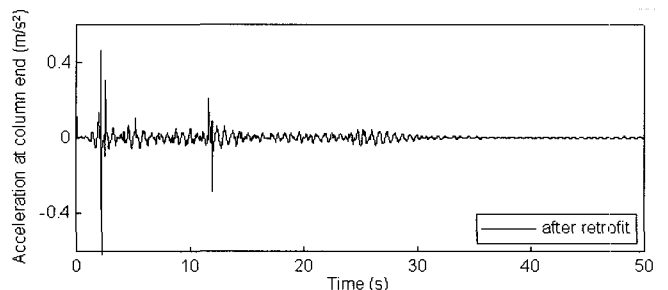
Typical responses at expansion joints of Bridge 2 are of interest and plotted in Fig. 7 to show the differences in structural behaviors in terms of relative displacement between right and left girders for the cases without and with considering gap and hook elements used in this study. The effect of restrains is significant and can be seen by comparing Figs. 7(a) and (b).

5. Fragility analysis of bridges

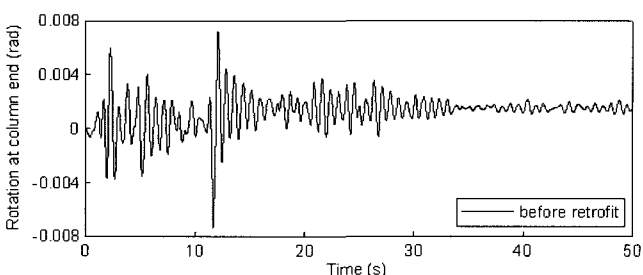
It is assumed that the fragility curves can be expressed



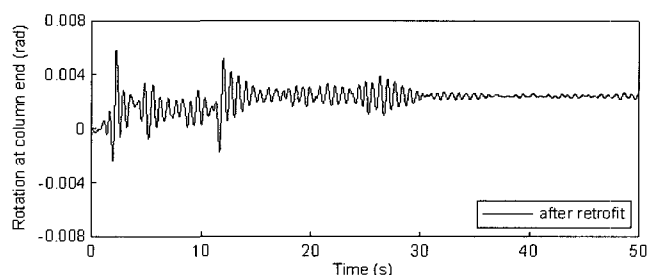
(a) Acceleration at column end before retrofit



(b) Acceleration at column end after retrofit

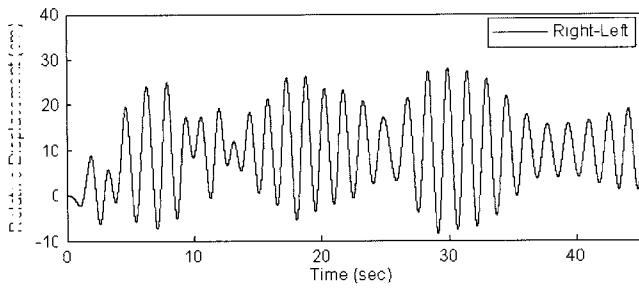


(c) Rotation at column end before retrofit

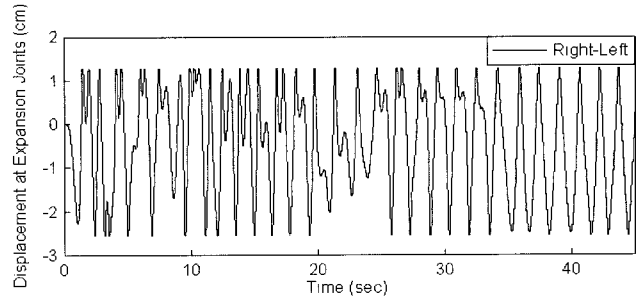


(d) Rotation at column end after retrofit

Fig. 6 Responses at column end of Bridge 1



(a) without Gap and Hook Elements



(b) with Gap and Hook Elements

Fig. 7 Displacement at expansion joints of Bridge 2

in the form of two-parameter lognormal distribution functions, and the estimation of the two parameters (median and log-standard deviation) is performed with the aid of the maximum likelihood method. A common log-standard deviation, which forces the fragility curves not to intersect, can also be estimated. The following likelihood formulation described by Shinozuka et al.⁽⁷⁾ is introduced for this purpose.

Although this method can be used for any number of damage states, it is assumed here for the simplicity that there are four states of damage from none to severe. A family of three fragility curves exists in this case where events E_1 , E_2 , E_3 and E_4 respectively indicate none, minor, moderate and major damage. $P_{ik} = P(a_i, E_k)$ in turn indicates the probability that a bridge i , selected randomly from the sample, will be in the damage state E_k when subjected to ground motion intensity expressed by $PGA = a_i$. All fragility curves are then represented

$$P_j(a_i; c_j, \zeta_j) = \Phi \left[\frac{\ln(a_i/c_j)}{\zeta_j} \right] \quad (2)$$

where $\Phi(\cdot)$ is the standard-normal distribution function, c_j and ζ_j are the median and log-standard deviation of the fragility curves for the damage states of "at least minor", "at least moderate" and "major" identified by $j=1, 2$ and 3 . From this definition of fragility curves, and under the assumption that the log-standard deviation is equal to ζ common to all the fragility curves, one obtains;

$$P_{D1} = P(a_i, E_1) = 1 - F_1(a_i; c_1, \zeta) \quad (3)$$

$$P_{D2} = P(a_i, E_2) = F_1(a_i; c_1, \zeta) - F_2(a_i; c_2, \zeta) \quad (4)$$

$$P_{D3} = P(a_i, E_3) = F_2(a_i; c_2, \zeta) - F_3(a_i; c_3, \zeta) \quad (5)$$

$$P_{D4} = P(a_i, E_4) = F_3(a_i; c_3, \zeta) \quad (6)$$

The likelihood function can then be introduced as

$$L(c_1, c_2, c_3, \zeta) = \prod_{i=1}^n \prod_{k=1}^4 P_k(a_i; E_k)^{x_{ik}} \quad (7)$$

where

$$x_{ik} = 1 \quad (8)$$

if the damage state E_k occurs in the i -th bridge subjected to $a = a_i$ and

$$x_{ik} = 0 \quad (9)$$

otherwise. Then the maximum likelihood estimates c_{0j} for c_j and ζ_0 for ζ are obtained by solving the following equations,

$$\frac{\partial \ln L(c_1, c_2, c_3, \zeta)}{\partial c_j} = \frac{\partial \ln L(c_1, c_2, c_3, \zeta)}{\partial \zeta} = 0 \quad (j=1, 2, 3) \quad (10)$$

by implementing a straightforward optimization algorithm.

5.1 Fragility Curves

Fig. 8 shows a typical fragility curve, based on 60 time histories, along with the 60 point pairs indicating whether the damage state was sustained or not. A total of 60 diamonds plotted on the two axes at $x_i=0$ for the state of 'no damage' and $x_i=1$ for the state of 'slight damage'.

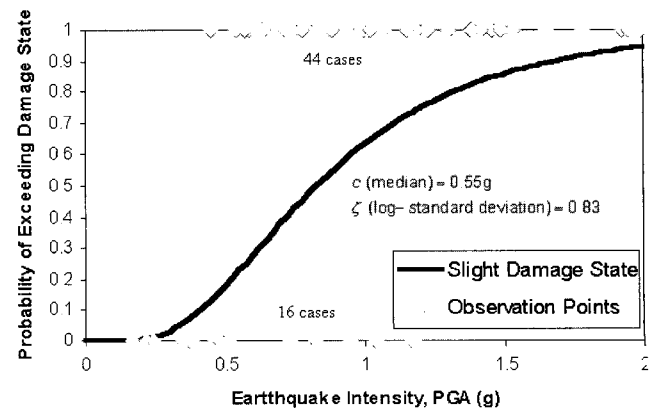


Fig. 8 Fragility curve for slight damage state

The corresponding fragility curves are derived on the basis of these diamonds in conjunction with Eqs. (2) through(10).

The fragility curves for Bridges 1 and 2 associated with these damage states are plotted in Figs. 9 and 10, respectively, for before and after retrofit as a function of peak ground acceleration. Note that the same log-standard deviation value for the pair of fragility curves in Figs. 9

and 10 is obtained by considering the two cases(before and after retrofit) together and calculating the optimal values from Eq. (10) for these fragility curves. This is because the bridge with jacketed columns is expected to be less vulnerable to ground motion than the bridge without column jacketing and, therefore, the pair of these fragility curves should not theoretically intersect.

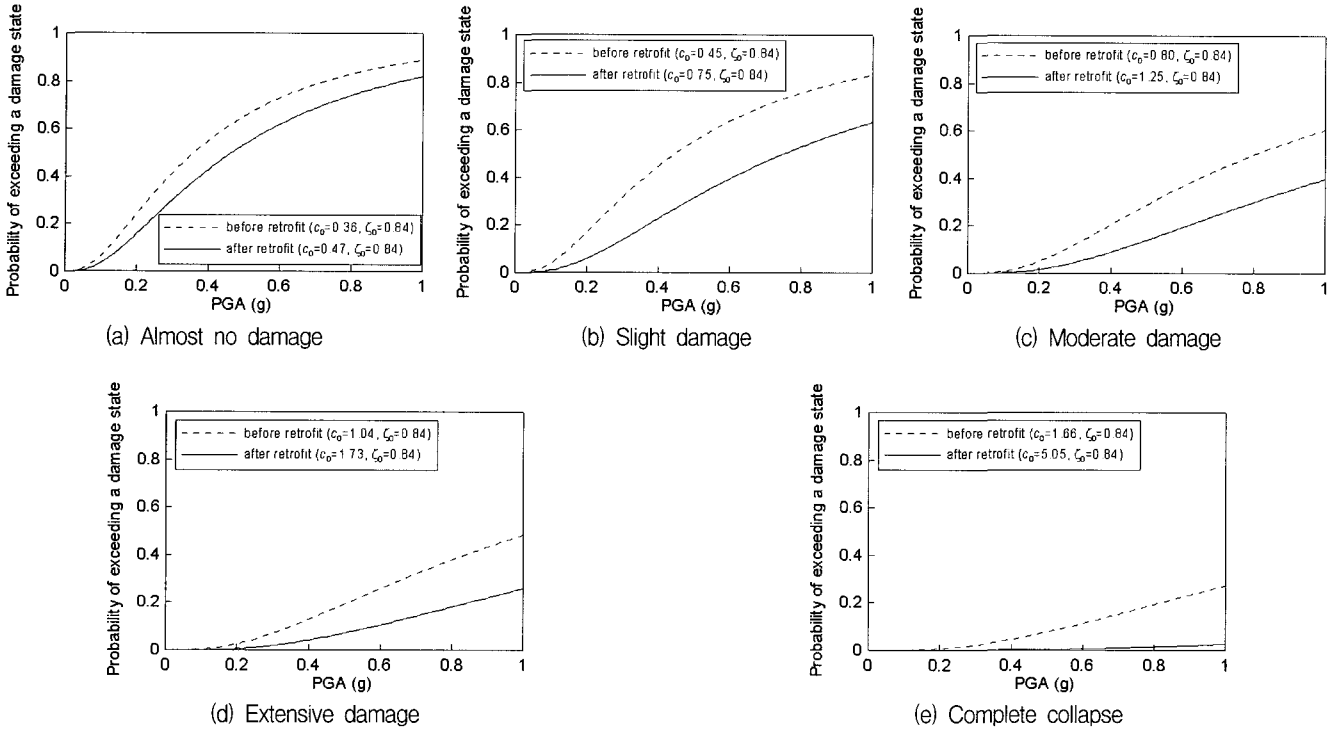


Fig. 9 Fragility curves of Bridge 1

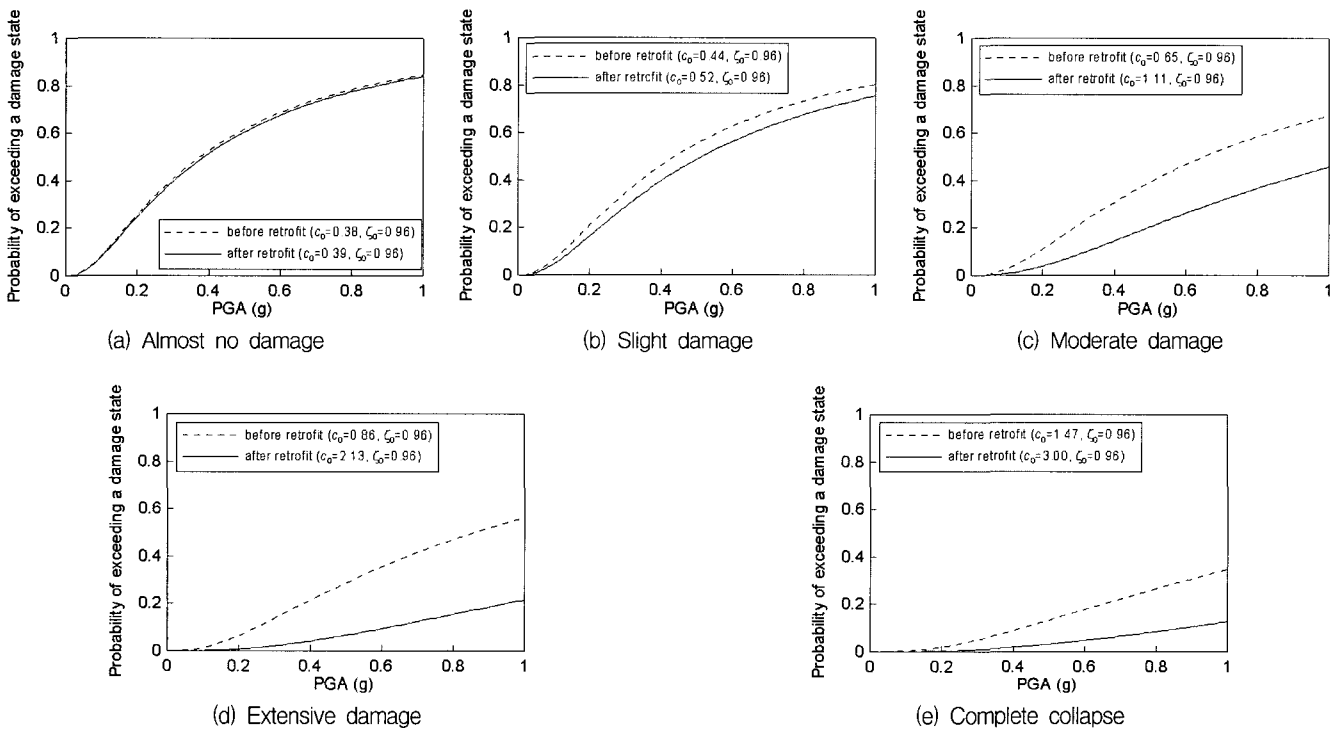


Fig. 10 Fragility curve of Bridge 2

5.2 Effect of steel jacketing

The damage state of a bridge in this study is defined by the maximum value of the peak ductility demands observed among all the column ends. In this context, comparison between the two curves in Figs. 9 and 10 indicates that the bridge is less susceptible to damage from the ground motion after retrofit than before. The simulated fragility curves demonstrate that, for all levels of damage states, the median fragility values after retrofit are larger than the corresponding values before retrofit. This implies the following: for Bridge 1, on average, there is a small number of damaged bridges after it has been retrofitted. Tables 3 and 4 list the number of damaged bridges both before and after retrofit for Bridge 1 and Bridge 2, respectively. The results in Tables 3 and 4 are consistent with the observation that the fragility enhancement is more significant for more severe states of damage. It shows that column retrofit greatly improves the seismic performance of bridges; Bridge 1 is up to three times less fragile (complete damage) and Bridge 2 is 2.5 times (extensive damage) less fragile after retrofit in terms of the median values.

The effect of retrofit is demonstrated by comparing the ratio of the median value of the fragility curve for retrofitted column to that of the unretrofitted column. This ratio is referred to as fragility "enhancement". Considering Bridges 1 and 2 with circular columns and corresponding sets of fragility curves before and after retrofit, the average fragility enhancement over these bridges at each state of damage is computed and plotted as a function of the state of damage. An analytical function is interpolated as "enhancement

curve" and is plotted through curve fitting as shown in Fig. 11. This curve shows 20%, 34%, 58%, 98% and 167% improvement for each damage state described on the x axis in Fig. 11.

It is assumed that the fragility enhancement obtained from this function also applies to the development of the fragility curves after the retrofit for the empirical fragility curves (Fig. 12) associated with expressway bridges in Los Angeles and Orange County, California subjected to the Northridge earthquake.

Assuming that Dutta and Mander's damage states (1999) are interchangeable with Caltrans definition so that "slight=minor", "moderate=moderate", "extensive=major" and "complete=collapse", three enhanced empirical fragility curves after retrofit for minor, moderate and major damage are plotted in Figs. 13, 14 and 15, respectively, for use in expressway network performance analysis.

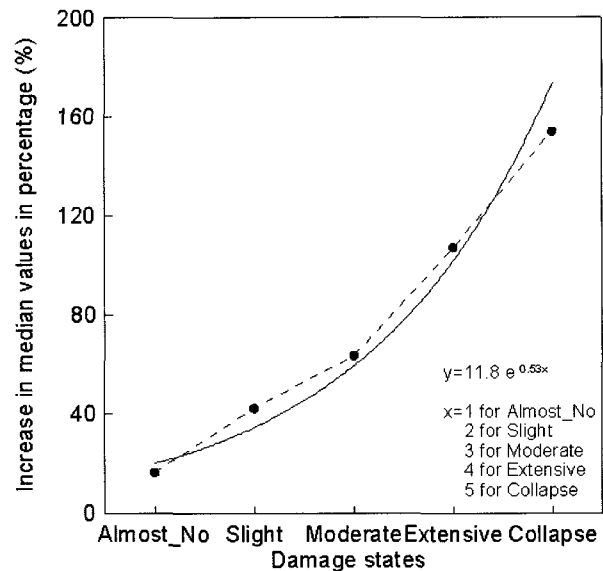


Fig. 11 Enhancement curve for circular columns with steel jacketing

Table 3 Number of damaged Bridge 1 (sample size=60)

Damage states	before retrofit	after retrofit
Almost no	56	53
Slight	51	44
Moderate	41	28
Extensive	34	15
Complete	17	2

Table 4 Number of damaged Bridge 2 (sample size=60)

Damage states	before retrofit	after retrofit
Almost no	51	50
Slight	47	41
Moderate	37	22
Extensive	30	10
Complete	14	4

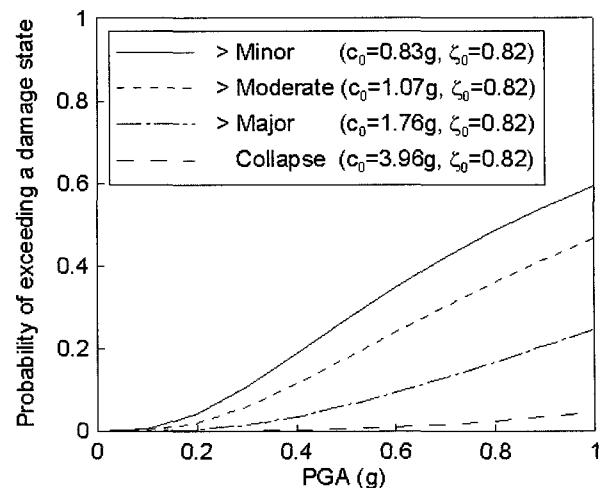


Fig. 12 Empirical fragility curves of Caltrans' bridges⁽⁹⁾

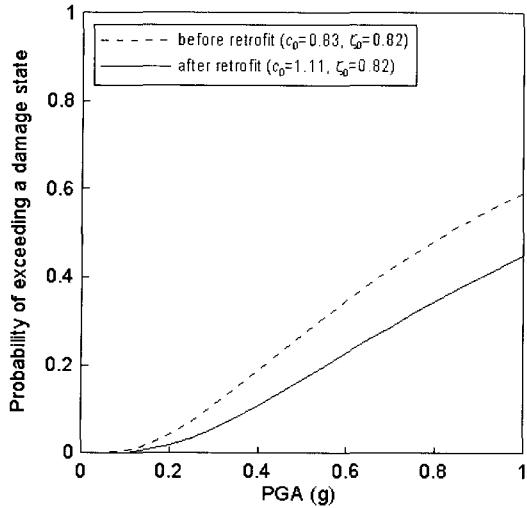


Fig. 13 Enhanced empirical fragility curves for Minor damage after retrofit

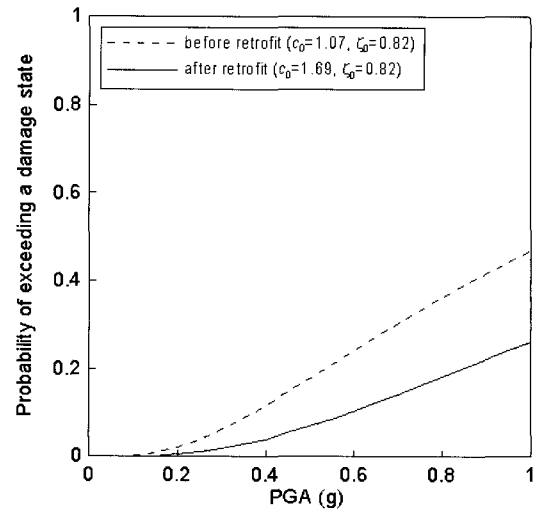


Fig. 14 Enhanced empirical fragility curves for Moderate damage after retrofit

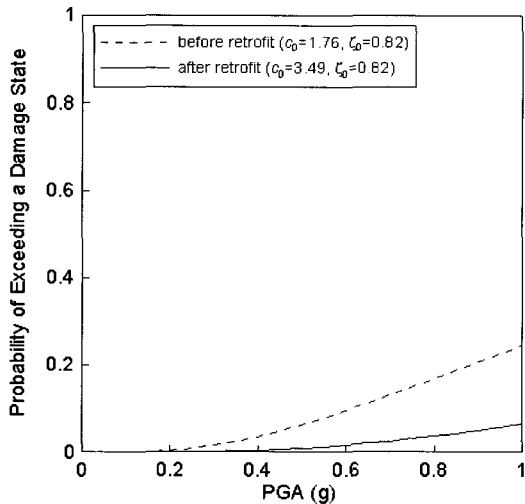


Fig. 15 Enhanced empirical fragility curves for Major damage after retrofit

(modeled as the hook element introduced in Fig. 3) designed for anchor force capacity in Fig. 17. These two figures show excellent improvement for both retrofit methods at expansion joints. However, this observation might not always apply, depending on the specific bridge characteristic. Further study is in progress.

6. Conclusions

This research presents a fragility analysis of two typical bridges in California before and after column retrofit with steel jacketing. The analytical fragility curves are constructed as a function of peak ground acceleration utilizing nonlinear dynamic analysis to investigate the effect of the column retrofit. Two-parameter lognormal distribution functions are used to represent the fragility curves by using the maximum likelihood procedure. Each event of bridge damage treated as a realization from a multi-outcome Bernoulli type experiment.

Analytical fragility curves computed for various damage

5.3 Fragility curves for retrofit with restrainers

Fragility curves for Bridge 2 are also developed to demonstrate the effect of retrofit at expansion joints by extending seat width in Fig. 16 and installing restrainers

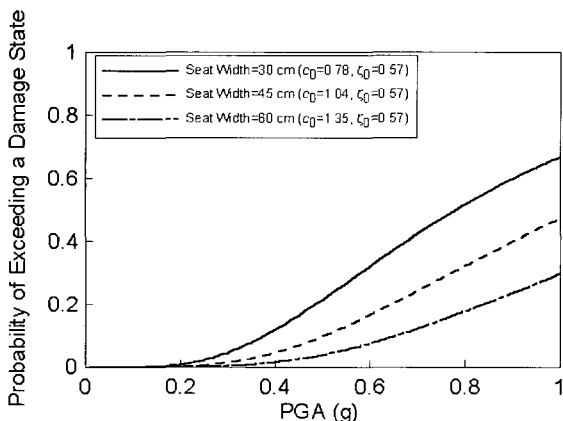


Fig. 16 Fragility curves for expansion joint retrofit by extension of seat width

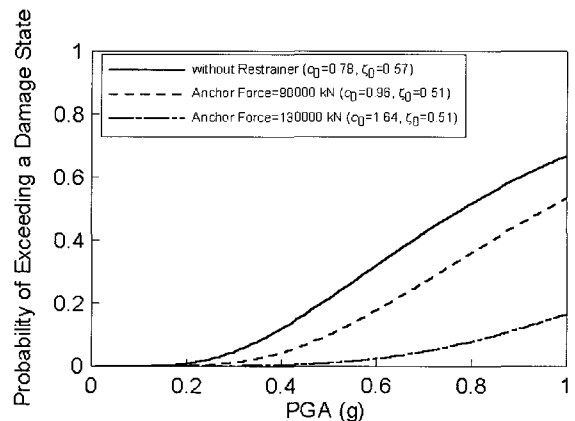


Fig. 17 Fragility curves for expansion joint retrofit by restrainers

states in this study make intuitive sense relative to the bridge's design, retrofit and performance in past earthquakes. This research provides information necessary to the design profession from performance design perspective, and paves the way for ensuing analysis to determine the level of enhancement of transportation network performance due to the retrofit. This research is thus beneficial to bridge engineering, transportation engineering and management professionals.

The following conclusions are drawn from the results of this study.

- (1) The simulated fragility curves after column retrofit with steel jacketing show excellent improvement (less fragile) when compared to those before retrofit by as much as three times based on median PGA values.
- (2) After retrofit, the number of damaged bridges substantially decreases; especially for severe damage states defined in this study.
- (3) An "enhancement curve" is proposed and applied to develop fragility curves after retrofit on the basis of empirical fragility curves.
- (4) Fragility curves developed for retrofit with restrainers provide useful information to the seismic design practice by quantifying the improvement due to retrofit.
- (5) On the strength of the results obtained in this and others studies, uncertainty analysis will be performed in relation to fragility characteristics.

References

1. Chai, Y. H., Priestley, M. J. N., and Seible F., "Seismic Retrofit of Circular Bridge Columns for Enhanced Flexural Performance," *ACI Structural Journal*, Vol. 88, No. 5, 1991, pp. 572-584.

2. Shinozuka, M., Kim, S. H., and Koshiyama, S., "Fragility Curves of Seismically Retrofitted Bridges with Column Jacketing," To be submitted for Publication, *Journal of Bridge Engineering*, ASCE, 2003b.
3. Priestley, M. J. N., Seible, F., and Calvi, G. M., *Seismic Design and Retrofit of Bridges*. John Wiley & Sons, Inc., 1996, pp. 270-273.
4. Shinozuka, M. and Kim, H. K., "Effects of Seismically Induced Pounding at Expansion Joints of Concrete Bridges," Accepted for Publication, *Journal of Engineering Mechanics*, ASCE, 2003a.
5. SAP2000 v.7.44 User Manual, Computer and Structure, CA, USA, 2002.
6. Koshiyama, S., "Calculation Moment-Rotation Relationship of Reinforced Concrete Member with/without Steel Jacket," Unpublished Report at University of Southern California, CA, USA, 2002.
7. Dutta, A. and Mander, J. B., "Seismic fragility analysis of highway bridges," *Proceedings of the Center-to-Center Project Workshop on Earthquake Engineering in Transportation Systems*, Tokyo, 1999.
8. Shinozuka, M., Kim, S. H., Yi, J. H., and Koshiyama, S., "Fragility Curves of Concrete Bridges Retrofitted by Column Jacketing," *Earthquake Engineering and Engineering Vibration*, Vol. 01, No. 2, 2002.
9. Shinozuka, M., Feng, M. Q., Kim, H. K., Uzawa, T., and Ueda, T., "Statistical Analysis of Fragility Curves," Technical Report at Multidisciplinary Center for Earthquake Engineering, 2001.